MODELING OF A TWO-STAGE MAGNETIC REFRIGERATOR WITH WAVY-STRUCTURE GADOLINIUM HEAT EXCHANGERS

D. Vuarnoz, A. Kitanovski, C. Gonin, O. Sari, P.W. Egolf

University of Applied Sciences of Western Switzerland
Institute of Thermal Sciences and Engineering
CH 1401 Yverdon-les-Bains, Switzerland

Corresponding author: Peter.egolf@heig-vd.ch

ABSTRACT

In a rotary magnetic refrigerator a porous ring is turning in and out of a magnetic field region. At the outlet the adiabatic demagnetization of the magnetocaloric material (refrigerant) produces the "cold energy". The induced cold is described by a corresponding discontinuous temperature decrease, known as adiabatic temperature difference. For such a machine a sophisticated physical model has been developed, based on a mapping of the magneto-thermodynamic problem from a cylinder onto two rectangles. In this model, in a basic centre cell, two coupled linear partial differential equations are solved, which have been programmed in the Modelica language. To determine the performance of a two-stage magnetic refrigerator, an ensemble of this new designed centre module and some other recently created auxiliary modules are coupled with standard components from a Dymola thermal library, as e.g. pumps, ordinary heat exchangers, tubes, pipes, etc. The operation of a magnetic refrigerator is simulated with numerous parameters. Steady state solutions are obtained to verify the coefficient of performance under stable operation conditions. Optimal running conditions – defined by maximal values of the coefficient of performance – are not presented in this article, but can now easily be obtained with the existing program. Finally, a regulation strategy is proposed and implemented into the Dymola-Modelica program.

1. INTRODUCTION

In the period between the discovery of the magnetocaloric effect by Warburg and its physical explanation by Weiss and Piccard, it already stimulated numerous ancient engineers and scientists, including the famous pioneers Tesla and Edison, to invent some machines based on this effect. Some of these inventions were devoted to energy conversion utilizing thermal heat sources from nature or industrial sites. Although the cryogenics community in a reasonable time could transfer this technique to investigate basic physics phenomena close to the point of absolute zero, at that time close to or room temperature applications were not judged to be competitive enough to beat machines with vapour-compression thermodynamic cycles. This was due to the lack of enough performing magnetocaloric materials and permanent magnets with sufficient good properties.

At the end of the last millennium, the "giant" magnetocaloric effect was discovered and started to reveal a realistic potential to open certain suitable refrigeration markets for the magnetic refrigeration technology.

Nowadays the literature on the field consists of a majority of studies dealing with the magnetocaloric effect (MCE) in materials. Also an increasing number of papers treat thermo-magnetic machine design and calculation, and a somewhat smaller number describes theoretical and numerical simulation work (see e.g. Ref. [1], [2] and [3]).

For example a thermodynamic model and related numerical simulations of the behaviour of a machine with a magnetocaloric wheel has been worked out by Egolf *et al.* [4]. Temperature mappings are obtained for both, material and fluid components of the rotor. More recently, Šarlah [5] performed a study with a comparison of

achievable performances of regenerators. As a main result, he shows formally the impact of the pressure loss versus the heat transfer coefficient on the main performance of the regenerator.

Engelbrecht *et al.* [6] used a NTU method to elaborate a full model on the prototype being a liquid AMRR system, with a particle bed built by the Astronautics Corporation of America. They compared the simulation results with experimental data of Zimm *et al.* [7]. An over prediction of loss is shown at low ratio of the thermal capacity of the flowing fluid to the thermal capacity of the matrix.

2. MAGNETIC REFRIGERATOR

2.1 The thermodynamic system

The investigated system is a domestic refrigerator – with two magnetocaloric generators coupled in a cascade – as shown in FIG. 1. Ideal operation conditions of the magnetocaloric generators are shown in two standard thermodynamic processes (see in FIG. 2).

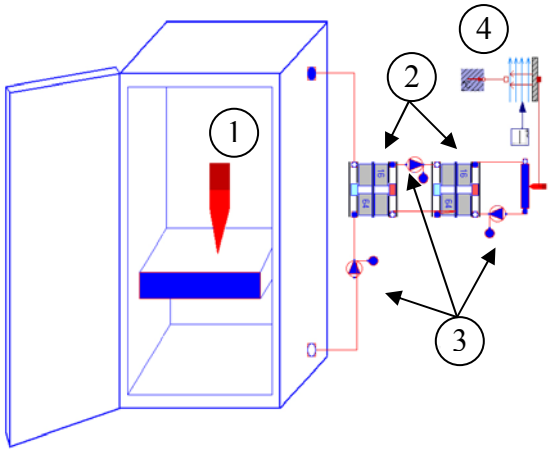

Figure 1. Schematic design of a magnetic refrigerator as implemented into the software Dymola. The main components of the system are: 1) Insulated fridge, 2) Magnetocaloric generators, 3) Pumps, 4) Hot heat exchanger, cooled by natural convection of ambient air.

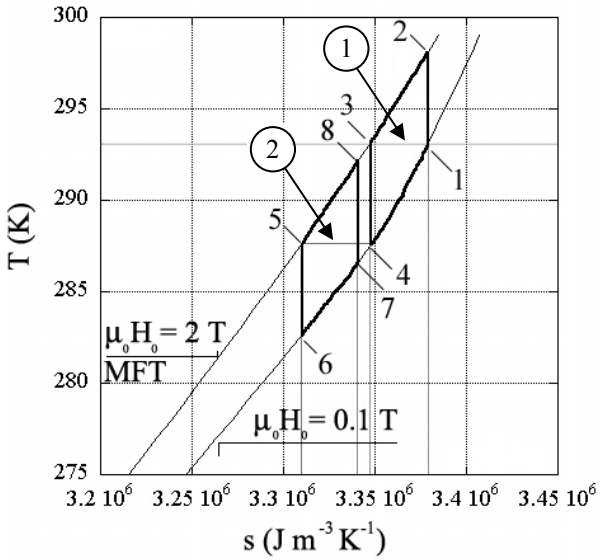

Figure 2. Representation of two Brayton cycles in a temperature versus specific entropy (*T,s*) diagram. It is worked out for gadolinium and has been taken from reference [8]. The symbol $\mu_0 H_0$ represents the intensity of the external magnetic field, which is applied.

The first cycle is the one denoted in figure 2 by number 1. A first step (1→2) is the magnetization from a magnetic field $H_0^{(1)}$ to $H_0^{(2)}$ of a porous solid magnetocaloric structure in a magnetic field. This process generates simultaneously a heating-up of the material. By introducing a fluid flow through it, the ring is cooled (2→3). After that it turns out of the magnetic field and by a demagnetization process (3→4) the magnetocaloric ring cools down. By contact with a fluid – which is cooled, because a porous structure can absorb a lot of heat in a short time – this part of the wheel is heated back to the initial stage (1). The two flows show opposite flow directions. The second stage, corresponding to the cycle denoted by number 2, operates by the same principle as the first one. Some compulsory conditions are required in order to correctly adjust the first magneto-thermodynamic cycle to the second one. In case of perfect heat transfer between the working fluids and the magnetocaloric ring – and in order to also fulfil the first law of thermodynamics – the energy transferred from the cold part of the first stage needs to be identical to the one coming from the warm part of the second stage. The surface area below the points 4→1 needs to be the same as the one limited by the segment 8→5. In the described specific case the total specific energy flux between the first and the second stage is 9'950 kJ/m^3. This case was worked out for gadolinium wheels and an ambient temperature of 293.15 K. The temperature link between the two cycles is between point 5, defined by the temperature level of point 4. Based on these considerations, the temperature T and the specific entropy s have been evaluated for all corner points of the two thermodynamic cycles. They are presented in Table 1.

Table 1: Temperature and specific entropy corresponding to the thermodynamic diagram shown in FIG. 2 for the two cycles of the cascade system.

First stage			Second stage		
point (FIG. 2)	s (J m^{-3} K^{-1})	T (K)	point (FIG. 2)	S (J m^{-3} K^{-1})	T (K)
1	3380130	293.15	5	3308696	287.53
2	3380130	297.15	6	3308696	282.35
3	3347233	292.31	7	3341686	286.96
4	3347233	287.49	8	3341686	292.15

2.2 The magnetic cooling modules of the magnetic refrigerator

In the magnetocaloric generators – designed for this modeling work – the magnetocaloric wheel contains four domains. These are the domains containing the magnetocaloric material, namely on the cold and on the hot side, and, furthermore, the corresponding fluid domains finely dispersed between the solid magnetocaloric material domains showing percolation in the mathematical sense.

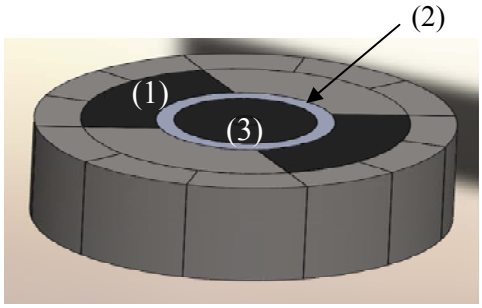

Figure 3. The main magnetic cooling element of a magnetic refrigerator is shown in this figure. It is of cylindrical type and shows an axial flow direction of the heat transfer fluid in two to each other opposite sides. The magnetic assembly is denoted by number (1), a rotating porous magnetocaloric ring by (2). This wheel is attached to an axel at position (3), which is not drawn in the picture (see also in Ref. [9]). This wheel is a slightly more complex one, containing two magnetic field and two zero-field regions.

3. PHYSICAL MODELING

The most complex module in a magnetic refrigerator is the magnetocaloric generator. The new developed module contains all the equations (algorithms) of the thermodynamic model presented in Chapt. 3.

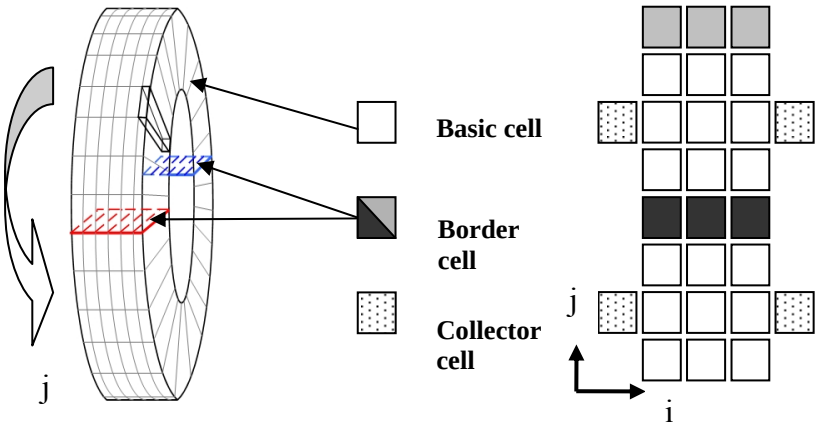

Figure. 4. The decomposition of the magnetocaloric ring into cells is presented. The left drawing shows a perspective view of the wheel, and on the right the 2-d assembly is outlined. Boarder cells do not represent any real domains. For each column of cells the vertical connection between the highest boarder cell and the lowest one – which is a basic cell – is not presented.

The physical modelling is described in detail in an earlier article found as reference [2]. It is based on two main simplifying assumptions:

1) The rotation frequency f of the ring is low compared to the inverse characteristic time of residence of a fluid lump flowing vertically (FIG. 3) and horizontally (FIG. 4) through the porous structure.

2) The heat conduction through the rotor in axial direction is negligible compared to the heat flux by convection.

The chosen object-orientated language is Modelica 2.2.1 with the commercialized interface Dymola 6.1. A similar mapping of a porous rotor has been used by another research group and is presented in Ref. [10]. These authors present an investigation of a desiccant cooling process with Dymola-Modelica. – FIG. 4 shows how in our case the rotor is decomposed into three different kinds of cells. They are discussed in the next three sub chapters.

3.1 Basic cells

Basic cells represent physically the part of the magnetocaloric rotor and describe processes from point No. 2→3, 4→1, 6→7, 8→5 in the thermodynamic cycle of FIG. 2. Deriving two times two coupled partial differential equations, which are presented in detail in Ref. [2], lead to the following well-conditioned algorithms for the centre cells:

$$T_{Fout} = \left(1 - \chi_F\right)\ T_{Fin} + \chi_F T_{Rin} \tag{1}$$

$$T_{Rout} = \left(1 - \chi_R\right)\ T_{Rin} + \chi_R T_{Fin} \tag{2}$$

T denotes the temperature and the index F the Fluid and R the Rotor matrix. The fluid temperature is handed over from an inlet to an outlet in horizontal direction and the rotor temperature identical in the vertical direction. The quantities χ_F and χ_R contain all physical properties of the fluid and the rotor material, respectively, and the heat transfer coefficients. They are defined as:

$$\chi_F = \frac{\alpha\ \Delta\phi}{\psi\ \delta\ \rho_R\ \omega_R\ c_H} \tag{3}$$

$$\chi_R = \frac{\alpha\ \xi\ \Delta z}{L\ \rho_F\ u_F\ c_{pF}} \tag{4}$$

The hydrodynamics of the fluid flow through the porous structure is mainly influenced by the geometrical quantities of the porous rotor. It is described in Ref [11], and it gives the pressure drop of the working fluid for the paths parallel to the axis of the cylindrical wheel. The pressure losses of the fluid flowing in and out of the magnetocaloric wheel are neglected:

$$\Delta p = \frac{1}{32}\rho_F u_F \nu L \frac{1}{{d_h}^2} \tag{5}$$

Basic cells were created with standard flow ports as offered by the Modelica thermal "FluidHeatFlow" library. In order to simplify the connection of cells, a small graphical difference in the connection ports in the icon of basic cells, located on the warm part, are distinguished by the ones on the cold part. But in our case the algorithms remain the same for the two cases.

3.2 Border cells

These virtual elements are related to real physical parts of the wheel (2-d plans are drawn for their representation (see e.g in FIG. 4)). In the border cells the reversible adiabatic temperature transitions, induced by the alternating magnetic field in the rotor structure, were implemented. They correspond in the Brayton cycle (shown in FIG. 2) to the two vertical lines 1→2, 3→4, 5→6 and 7→8. The adiabatic temperature change, as a function of the magnetocaloric material temperature and due to the magnetic field change, was determined by mean field theory calculations (results were taken from Ref. [8]). For gadolinium the specific heat capacity is shown in FIG. 6 with its curve fittings and the heating and cooling process – represented by the adiabatic temperature differences – are shown in FIG. 7. In this second case the curve fittings are not shown, but by exponential functions an excellent representation of the curves could be obtained.

3.3 Thermal diffusion in the rotor

A virtual loop in the *j* direction (vertical direction in FIG. 4) is required for the transfer of correct temperatures to lines of basics cells located just after the boarder cell alignment's (rotor connectors). The frequency of the adiabatic temperature change imposes here a virtual volumetric flow of:

$$\dot{V}_R^{(fictive)} = \frac{f\, m_R\, c_{pR}}{\rho_F^{(fictive)} c_{pF}^{(fictive)}} \tag{6}$$

The fluid viscosity of the virtual fluid streaming in this loop is set to zero with the objective to not induce any friction losses.

3.4 Sensitivity on the mesh sizes

The assembly of home-made cells (basic cells, border cells) together with numerous standard modules, e.g. for pumps, heat sources and flowPorts, from the thermal "FluidHeatFlow" library, can be assembled to obtain a magnetocaloric generator module. Such a module is shown in FIG. 4.

In order to verify the sensitivity of the model on the maximal numbers of cells in *i* and *j* direction, the dependence on the numbers is investigated. For a variation of the numbers of basic cells from 2 to 8, to 256 and to 1024 cells, the response of the temperature of an air flow at the outlet of the cold domain was plotted and is shown in FIG. 5.

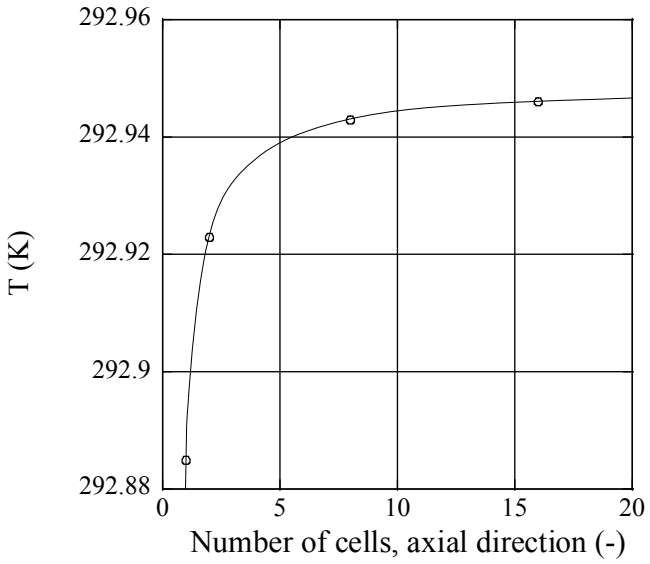

Figure 5. The fluid temperature at the outlet of the cold region of a one-stage machine is shown. With an increasing number of cells the temperature systematically increases and converges. If the number of cells in the axial direction is 16 or more, then the temperature does not change remarkably anymore. The parameters for these simulations are also those presented in Appendix 1. The finally chosen size of the model of a magnetocaloric generator is a cell pattern containing 1024 basic cells, 2 times 16 boarder cells and four collector cells. For a cascade system two times the number of these cells are present. Each cell contains a number of equations, which leads to a large calculation task demanding high computing power. All implemented parameters are shown in Appendix 1.

4. SET-UP OF PARAMETERS

4.1 The magneto-thermodynamic generator

The two stages of the cascade process are actually identical. The thermo-physical properties of the rotor material are those of gadolinium. The reason is that its properties for this model substance are theoretically calculable and, therefore, are also well defined. The parameters of the geometry of the porous wheel are also clearly defined, and they have been carefully chosen in order to have a "realizable" rotor with a package degree of 70 %. An external magnetic field is assumed to have a magnitude of 2 Tesla in the magnetized areas of the porous ring. The important parameters characterizing the thermo-magnetic generator are listed in Appendix 1.

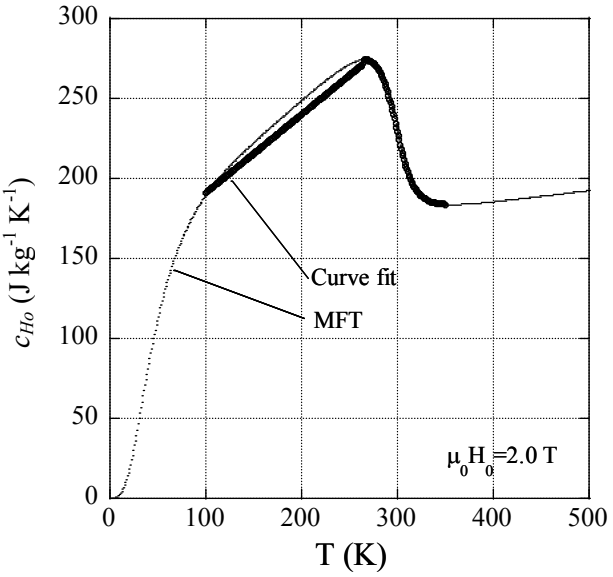

Figure 6. The specific heat of gadolinium for an external field of 2 T is shown as a function of temperature. Two curve fittings were applied in the ranges 100 K $\rightarrow T_C$=293 K and $T_c \rightarrow$350 K with approximations by a linear and a sinus function (MFT=mean field theory).

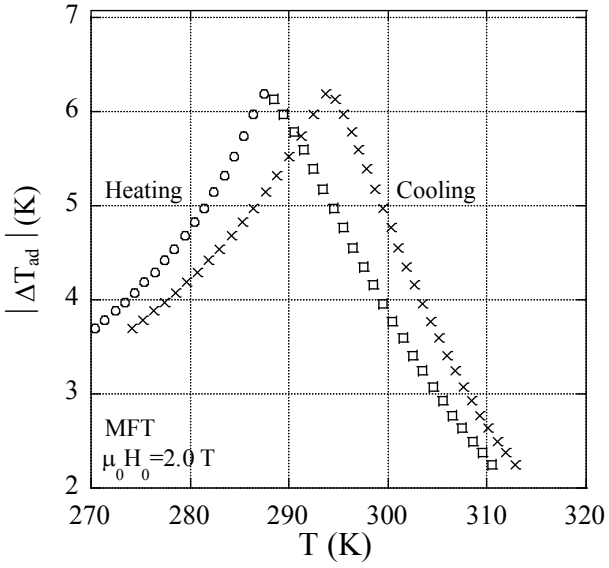

Figure 7. The adiabatic temperature change of gadolinium for an increase of the external magnetic field from 0.1 T up to 2 T is presented. Curve fittings to the points shown in this figure were performed by different exponential functions.

4.2 The parameters characterizing the fluid

In all investigated cases air is the working fluid. The physical properties of this fluid applied are also reported in Appendix 1. The mass flow through the porous ring leads to a local velocity in the structure of approximately u_F=2 m/s.

4.3 Simulation parameters

The full model was numerically checked and shows good results when parameters are set-up with appropriate values. Some numerical instability appears in some rather rare unproblematic circumstances. Grid increment distances and other auxiliary parameters are also presented in Appendix 1.

4.4 Listing of parameters

The full model of the two-stage cascade refrigerator contains 97'583 equations. Furthermore, parameters of a non-optimized system (but at least being close to reality) are listed in Appendix 1. The thermal load in the fridge appliance is composed of 10.5 kg chocolate.

5 SIMULATION RESULTS

After the generator module was built and the entire system was put together by connecting two new modules correctly with others from standard libraries, the parameters were chosen and then the simulation process started. Temperatures at each inlet and outlet of the second stage module and in the appliance were monitored. They start to cool down from the ambient temperature to their steady state as shown in FIG. 8.

The investigated refrigeration unit with a two-step cascade working with a mass of totally 536 g of Gd cools 10.5 kg chocolate 7 K in approximately 14 hours.

The coefficient of performance (*COP*) of each stage can be determined with the help of the *T-S* diagram (see FIG. 2) by applying a method presented in Ref. [12]. The thermodynamic *COP* of the first stage is 66 and of the second 60. The second stage is less performing, because it is operating more distant from the Curie temperature of gadolinium than the first one.

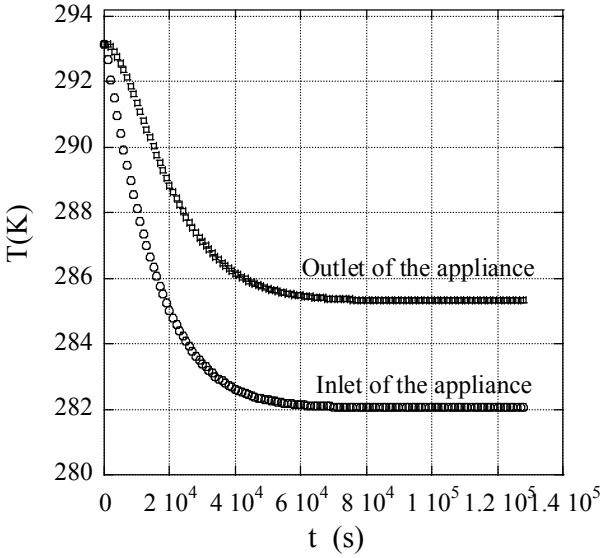

Figure 8. Time evolution of the temperature of the working fluid at the inlet and outlet of the magnetic refrigerator appliance modelled according to the schematic drawing shown in FIG. 1. A perfect heat transfer is assumed to occur between the charge, given by a Swiss chocolate load, and the air in the refrigerator. The inside temperature of the appliance is identical to the one of the air flowing out of the equipment. The refrigerator is assumed to have a standard insulation and no door openings were taken into consideration. The time to reach the steady state temperature is rather large and as a result a higher filling of magnetocaloric material is proposed to increase the power of this environmentally benign machine.

After a simple numerical cooling experiment, a practical operation of a realistic magnetic household refrigerator was performed. The refrigerator possesses a simple regulation system, which guarantees a certain stability of the inside air temperature by an alternating sequence of an "ON" and "OFF" mode.

Figure 9. On the right-hand side a simulation of a regulated two stage magnetic refrigerator operating with gadolinium is presented. The inlet temperature evolution of the air in the cabinet during the "OFF" mode shows the typical exponential decay as it is expected to occur in such a thermodynamic machine with a thermal inertia and heat transfer losses.

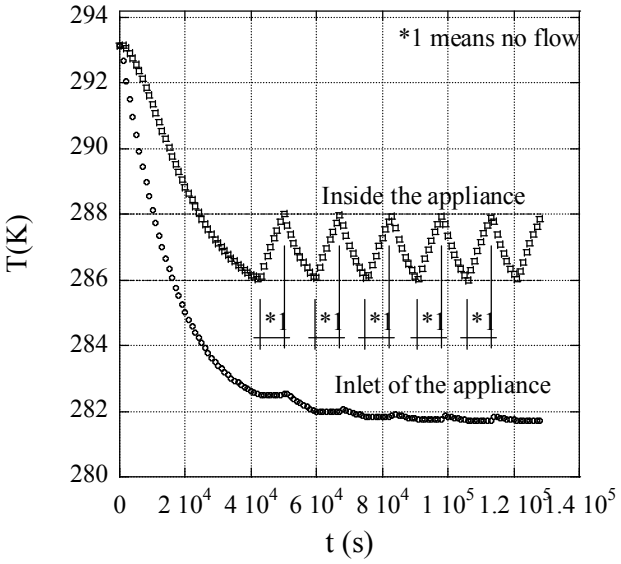

6. CONCLUSIONS AND OUTLOOK

In this article an informatics tool to optimize magnetic refrigerators is presented. It contains a user-friendly commercialized interface Dymola, where by drag and drop methods a refrigerator can be easily built together and modified. For example, immediately two stages of a magnetic refrigerator could be supplemented by a third one. It is just these magnetic generator modules, which have been recently developed by scientists of the Thermal Science and Engineering Institute in Yverdon, Switzerland, that make it now possible to apply the Dymola-Modelica software tools to magnetic refrigeration, heat pumping and energy conversion. Programming in this modern software is performed by the application of the object-oriented language Modelica. The parameters have not yet been determined by solving the numerical method "Optimization Problem", where the parameters are determined in such a manner that a final quantity is optimized. Under given operation characteristics such an optimization (minimization) parameter could for example be the magnetic mass of the refrigerator, because of a relatively high price of the magnets assembly, or the maximisation of the *COP* or even both criteria. Based on the calculation results the magneto-thermodynamic *T-s* diagram containing the cycles of the two stages could be reconstructed. The first stage is more efficient, because it operates in a domain closer to the Curie temperature of gadolinium than the second one. By applying some alloy and the layered bed technique, here a further optimization could be obtained. If a gadolinium filling of 540 g of magnetocaloric material is realized then a two-stage cascade refrigerator, as investigated in this work, can cool down in 14 hours 10.5 kg chocolate to the optimal storage temperature. Further improvements and the optimisations of this and similar machines are at present under performance.

ACKNOWLEDGEMENTS

The authors are grateful to the Swiss Federal Office of Energy for its financial support and to the Gebert Rüf Stiftung and the Hes-so foundation for continuous interest in our work. We also thank M. Delessert, Y. Borgeaud and M. Meinen for good collaboration. Furthermore, we express our gratitude to S. El Maudni El Alami for his internship work on this topic. Helpful remarks by W. Maurer and B. Frei are appreciated.

NOMENCLATURE

d	Diameter (m)	*in*	Inlet
f	Frequency (s^{-1})	*out*	Outlet
T	Temperature (K)	*ad*	Adiabatic
s	Specific entropy ($J\ m^{-3}\ K^{-1}$)		
B	Magnetic field induction (T)	*Greek*	
z	Length (m)	χ	Characteristic number (-)
p	Pressure (Pa)	α	Heat transfer coeff. ($W\ m^{-2}\ K^{-1}$)
c	Specific heat ($J\ kg^{-1}\ K^{-1}$)	ξ	Characteristic geom. quantity (m)
CUP	Chocolate Unit Plate, equiv. 100 g	δ	Characteristic geom. quantity (m)
v	Velocity ($m\ s^{-1}$)	Δ	Difference
		ψ	Porosity (–)
subscript		ρ	Density ($kg\ m^{-3}$)
F	Fluid	Φ	angle
h	hydraulic	υ	Viscosity ($m^2\ s^{-1}$)
R	Rotor		

APPENDIX

Appendix 1. Parameters as basis of the performed numerical simulations are shown in this table.

Quantity	Symbol	Value	Unit		Quantity	Symbol	Value	Unit
External diameter	d_0	0.1	m		Nb. mesh hor.	i	16	-
Inner diameter	d_1	0.08	m		Nb. mesh ver.	j	64	-
Lenth	L	0.04	m		Intervals print	*int*	128	-
Porosity	ψ	30	%		Precision	*prec.*	0.001	
Density rotor	ρ_R	7900	$kg\ m^{-3}$		Integrator step	*FIS*	0.5	s
Frequency rotor	f	0.35	Hz		Start time	t_0	0	s
Heat transfer coeff.	α	210	$W\ m^{-2}K^{-1}$		Stop time	t_{stop}	12800	s
Volume flow rotor	$\dot{V}_R$	0.0028	m^3s^{-1}		Therm. resist. rotor	R_{tot}	1.0378	$K\ W^{-1}$
Intensity low ext. field region	H_0	0.1	T		Ambient temperature	T_{amb}	293.15	K
Intensity high ext. field region	H_1	2.0	T		Heat transfer coefficient	α_{Nat}	5	$Wm^{-2}K^{-1}$
Hyd. diameter	d_h	$4.67\ 10^{-4}$	m		Volume flow	$\dot{V}$	0.002	m^3s^{-1}
Density	ρ_{Air}	1.149	$kg\ m^{-3}$		Charge	*CUP*	100	g
Viscosity	υ	$16.3\ 10^{-6}$	m^2s^{-1}		Spec. heat chocolate	c_{pchoco}	2000	$J\ kg^{-1}K^{-1}$
Specific heat capacity	c_{pair}	1007	$J\ kg^{-1}\ K^{-1}$		Dimension	*a*b*c*	0.3*0.35*0.4	m
Viscosity rotor loop	υ_R	0	$m^2\ s^{-1}$		Intitial Temperature	T_{ini}	293.15	K

REFERENCES

1 Gschneidner K.A. Jr, Pecharsky V.K., and Tsokol A.O., Recent developments in magnetocaloric materials, Institute of Physics Publishing, Rep. Prog. Phys. 68, pp. 1479-1539, 2005.

2 Kitanovski A., Egolf P.W., Gendre F., Sari O., Besson Ch., A rotary heat exchanger magnetic refrigerator, Proceedings of the First International Conference on Magnetic Refrigeration at Room Temperature, (Editor P.W. Egolf), ISBN 2-913149-41-3, Montreux, Switzerland, 27-30 September 2005, pp. 297-307.

3 Šarlah A., Poredos A., Dimensionless numerical model for determination of magnetic regenerator's heat transfer coefficient and its operation. Proceeding of the Second International Conference on Magnetic Refrigeration at Room Temperature, (Editor A. Poredos), ISBN 978-2-913149-56-4, Portoroz, Slovenia, 11-13 April 2007, pp. 419-426.

4 Egolf P.W., Sari O., Gendre F., Close-to-Carnot-cycle magnetic refrigerators and heat pumps: Analytical machine design and optimization. Proceedings of the Jubilee XX NMMM (New Magnetic Materials of Microelectronics) Conference, Russian Association of Magnetism, Lomonosov State University, Moscow, 12-16. June, AII-02, 2006.

5 Šarlah A. Thermo-hydraulic properties of heat regenerators in magnetic refrigerator. Ph D Thesis, Faculty of Mechanical Engineering of the University of Ljubljana, 2008.

6 Engelbrecht K.L., Nellis G.F., Klein S.A., Comparing modelling predictions to experimental data for AMRR systems. Proceeding of the Second International Conference on Magnetic Refrigeration at Room Temperature, (Editor A. Poredos), ISBN 978-2-913149-56-4, Portoroz, Slovenia, 11-13 April 2007, pp 349-357.

7 Zimm C., Auringer J., Boeder A., Chell J. Russek S., Sternberg A., Design and initial performance of a magnetic refrigerator with a rotating permanent magnet. Proceeding of the Second International Conference on Magnetic Refrigeration at Room Temperature, (Editor A. Poredos), ISBN 978-2-913149-56-4, Portoroz, Slovenia, 11-13 April 2007, pp 341-347.

8 Rosensweig R. E., Gonin C., Kitanovski A., Egolf P.W, Magneto-thermodynamic charts of gadolinium for magnetic refrigeration (in preparation).

9 Egolf P.W., Kitanovski A., Vuarnoz D., Gonin C., Swinnen T., Repetti P, Orita A., Beney J.L., Magnetische Wärmepumpe mit Erdwaerme-Quelle: Optimierter Prototyp, BFE project, Projekt-/Vertrags-Nummer 100'873/152'928, Jahresbericht 2008.

10 Casa W., Proelss K., Schmitz G. Modelling of desiccant assisted air conditioning systems, Proceedings of the 4th International Modelica Conference, Hamburg, Germany, 7-8 March 2005.

11 Egolf P.W., Accubloc – Regenerativer Wärmeübertrager mit stationären Speichern. Final report, EMPA, Dübendorf, 1999.

12 Vuarnoz D., Kitanovski A., Diebold M., Egolf P.W., A magnetic heat pump with porous magnetocaloric material, Physica Status Solidi C, ISSN 1610-1634, Vol. 4, No. 12, pp. 4552-4555, 2007.